J Electr Eng Technol.2018; 13(4): 1459-1473
http://doi.org/10.5370/JEET.2018.13.4.1459

ISSN(Print) 1975-0102
ISSN(Online) 2093-7423

Coordinated Voltage Control Scheme for Multi-Terminal Low-Voltage DC Distribution System

Trinh Phi Hai*, Il-Yop Chung†, Taehoon Kim and Juyong Kim****

Abstract – This paper focuses on voltage control schemes for multi-terminal low-voltage direct current (LVDC) distribution systems. In a multi-terminal LVDC distribution system, there can be multiple AC/DC converters that connect the LVDC distribution system to the AC grids. This configuration can provide enhanced reliability, grid-supporting functionality, and higher efficiency. The main applications of multi-terminal LVDC distribution systems include flexible power exchange between multiple power grids and integration of distributed energy resources (DERs) using DC voltages such as photovoltaics (PVs) and battery energy storage systems (BESSs). In multi-terminal LVDC distribution systems, voltage regulation is one of the most important issues for maintaining the electric power balance between demand and supply and providing high power quality to end customers. This paper focuses on a voltage control method for multi-terminal LVDC distribution system that can efficiently coordinate multiple control units, such as AC/DC converters, PVs and BESSs. In this paper, a control hierarchy is defined for undervoltage (UV) and overvoltage (OV) problems in LVDC distribution systems based on the control priority between the control units. This paper also proposes methods to determine accurate control commands for AC/DC converters and DERs. By using the proposed method, we can effectively maintain the line voltages in multi-terminal LVDC distribution systems in the normal range. The performance of the proposed voltage control method is evaluated by case studies.

Keywords: Multi-terminal LVDC distribution system, Voltage control, Multiple AC/DC converter control, Distributed energy resources, Voltage sensitivity analysis.

1. Introduction

With the recent development of power electronics technology, most electric loads now consume electrical energy in the form of direct current (DC) in the middle or final stage of their power converters. In addition, DC power is also used for the power generation of distributed energy resources (DERs). Low-voltage DC (LVDC) distribution systems are a new type of power distribution technology that can directly connect DC generators to DC loads at low voltages near electricity customers.

Recent studies have shown that LVDC systems are more economical than traditional alternating current (AC) distribution systems in certain circumstances [1-3]. Moreover, LVDC distribution systems can efficiently host multiple DERs such as renewable energy resources and energy storage systems (ESSs), through power-electronic converters that can effectively control power system parameters. Another advantage of LVDC systems is that DC systems do not have parameters such as frequency, phase angle, or reactive power so that it is possible to connect different types of DC sources without synchronization procedure [4].

Over the past decade, the Korea Electric Power Corporation (KEPCO) has been studying the application and operation of LVDC distribution systems in South Korea [5-6]. Based on the successful demonstration of an LVDC system in Finland [3], KEPCO has been pursuing research on the economic feasibility and relevant system design of LVDC systems. In 2015, KEPCO launched a new research project to develop an LVDC distribution system test facility in the Gochang Power Testing Center located in Jeonnam Province, South Korea. Fig. 1 shows the LVDC testing simulator in Gochang that contains many kinds of DERs, such as PVs, wind turbines (WTs), BESSs, diesel generators, combined-heat-and-power (CHP) simulators as well as AC and DC loads. All the DERs and loads are connected to the network through power electronic devices. The main AC/DC converters interconnect the LVDC distribution system to 22.9 kV medium voltage AC grid.

Similar to the Finnish system [3], the LVDC testing simulator is designed as a bipolar system whose rated voltage is ±750 V_{DC}. The simulator employs many disconnecting switches (DSs) that can remotely configure various network topologies, such as radial, loop, and mesh-type power distribution networks.

† Corresponding Author: School of Electrical Engineering, Kookmin University, Korea. (chung@kookmin.ac.kr)
* School of Electrical Engineering, Kookmin University, Korea. (trinhphihai@gmail.com)
** Korea Electric Power Research Institute (KEPRI), Korea. (nobleman@kepco.co.kr, juyong.kim@kepco.co.kr)
Received: November 22, 2017; Accepted: February 11, 2018

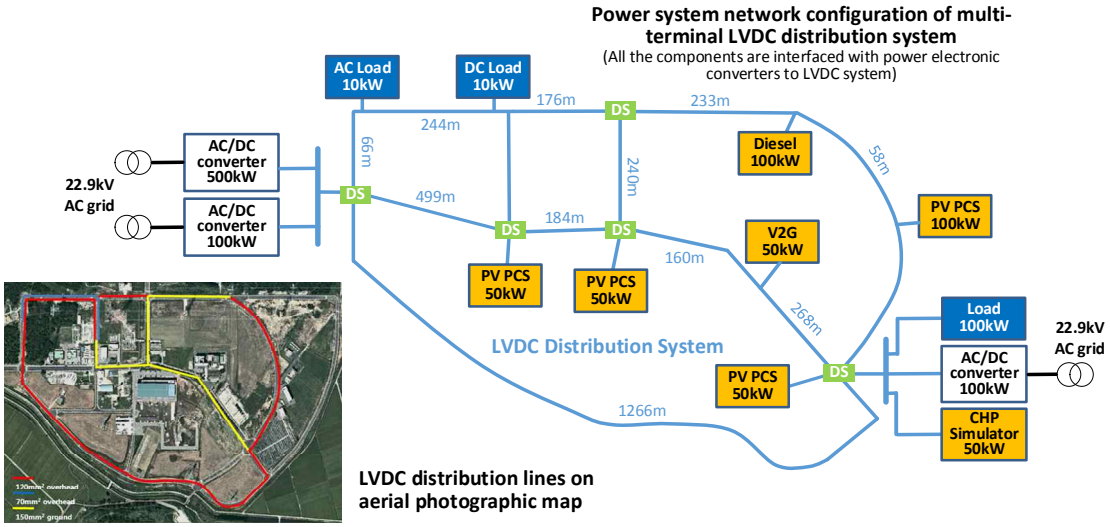

Fig. 1. Configuration of LVDC testing simulator in Gochang, South Korea

In the Gochang project, KEPCO plans to install multiple AC/DC converters so that the LVDC system can have multiple points of connection with other distribution or transmission systems. This configuration is called a multi-terminal LVDC distribution system. Multiple AC/DC converters can exchange electric power with other AC networks so that the system reliability can be significantly improved. In addition, a multi-terminal LVDC distribution system can allow power exchange between unsynchronized AC distribution systems, thus increasing system stability by preventing cascading failures.

There have been research studies on multi-terminal DC systems, but most of them focused on medium- or high-voltage transmission systems. [7-9] explain the advantages of multi-terminal medium-voltage DC (MVDC) systems in terms of efficiency, reliability, and flexibility. Some researchers have applied a multi-terminal DC system to the concept of the multi-microgrid [10] and the parallel connection of multiple renewable energy sources using voltage source inverters [11]. [12] applied the concept of the multi-terminal DC system to increase the rating and short circuit ratio of the system.

Compared to MVDC or high-voltage DC (HVDC) systems, LVDC distribution systems can be easily affected by voltage fluctuations caused by load variation or DER integration. Voltage regulation can limit the size and rating of LVDC distribution systems [13]. In addition, in DC systems, voltage is directly linked to active power and energy. Furthermore, in multi-terminal LVDC distribution systems, voltage control is more complicated due to multiple power flow paths. Therefore, voltage control in multi-terminal LVDC systems is important to maintain normal system conditions and stabilize power supply and demand.

This paper proposes a sophisticated voltage control method for multi-terminal LVDC systems that coordinates multiple AC/DC converters and DERs. First, this paper proposes a method to coordinate multiple AC/DC converters. To this end, we propose two methods, which are referred to as the numerical iterative computation method and the linear equivalent circuit method, to accurately calculate the control commands of AC/DC converters in multi-terminal LVDC distribution systems. We then compare the performance of the two methods in terms of accuracy and computational burden. This paper also proposes a voltage control scheme by coordinating multiple DERs such as PV panels and BESSs scattered in multi-terminal LVDC distribution systems. The proposed method considers the priority for types of DERs as well as the voltage sensitivity factor (VSF) for the active power injection of each DER.

The proposed voltage control algorithm can be implemented in hierarchical control architecture based on multi-agent system (MAS) that includes a supervisory master agent and local agents. Local agents are designed to produce time-synchronized measurement data such as voltage, current and power in local distribution lines. Local agents can also exchange measurement data with adjacent agents to estimate power system data for unmonitored buses. The control algorithms of local agents can be perfectly implemented in 32-bit microcontroller-based hardware that can be easily embedded into remote terminal units (RTUs) or advanced metering infrastructure (AMI) devices. We are developing a prototype voltage control system for Gochang LVDC system with dedicated communication protocol and middleware to implement MAS-based coordinated control platform.

2. Voltage control in LVDC distribution system

2.1 Conventional voltage control methods

Voltage regulation is an important issue in the design and operation of distribution systems. The objective of voltage regulation is to maintain the voltage profile of the

distribution system within a predefined range, which is typically defined as ±5% range of the nominal voltage [14-15]. There have been previous studies on voltage control schemes for LVDC distribution systems [16-18]. However, most of them focused on small-scale DC systems with limited service areas.

[16] focused on the voltage control of a radial LVDC distribution system with the injection power control of DERs. The authors showed that the VSF could be defined as the ratio of the voltage change at a specific bus over the injected power of the DER at another bus. Then, they proposed a simplified method to calculate the VSFs for a radial LVDC distribution system. Their method can quickly and accurately calculate VSFs, but it is confined to radial distribution systems.

[17] provided a systematic approach for the voltage control of a LVDC distribution system including multiple DERs. Their method consists of two sequential stages: the output voltage control of AC/DC converters in the first stage and the power control of DERs in the second. This sequential control method is similar to the voltage control method involving the cooperation of tap-changing transformers and static voltage compensators (SVCs) in the AC distribution system, which is familiar to the system administrators and operators. However, to calculate the control command of the AC/DC converters and DERs, the authors neglected the nonlinear characteristics of constant power loads and assumed the distribution system as a linear system.

[18] considered the LVDC distribution system nonlinear and compared the results with [17]. This paper provides the detailed nonlinear equations to calculate the control commands for the AC/DC converters and DERs.

This paper continues the discussion of voltage control in the [18] and extends the scope of the target system to multi-terminal LVDC distribution systems that consist of multiple AC/DC converters. Because of the existence of multiple AC/DC converters, this paper proposes a method to coordinate the AC/DC converters. In addition, we consider a ring-type distribution system that has multiple paths power flow paths.

2.2 Voltage regulation issues in multi-terminal LVDC distribution system

In a multi-terminal LVDC distribution system, the voltage profile becomes more complicated than in a conventional radial distribution system because there can be multiple power flow paths to loads. Moreover, if there are multiple DERs in the middle of the distribution lines, electric power can flow in the opposite direction to the grids. The more complex the system configuration (e.g. loop- or mesh-type networks), the more difficult it becomes to predict the power flow of the system.

To examine practical voltage profiles, we use a loop-type multi-terminal LVDC distribution system for a test system, which is illustrated in Fig. 2(a). The test system consists of two AC/DC converters, PVs, BESSs and loads. The AC/DC converters connect the LVDC system with upper-level grids and meet the load demand via load-following action by controlling the terminal voltage constantly. DERs such as PVs and BESSs can be installed in the middle of the LVDC distribution lines.

Fig. 2(b) illustrates an example of a voltage profile of the test multi-terminal LVDC distribution system under a specific loading and generation condition. In particular, Fig. 2(b) shows that overvoltage (OV) and undervoltage (UV) problems can occur simultaneously in a multi-terminal LVDC distribution system. To obtain this abnormal condition, we assume a situation with maximum DER generation in the upper distribution line (between buses 1 and 4) and a heavy loading condition in the lower line (between buses 6 and 9). Fig. 2(b) shows two voltage profile curves after the AC/DC converter control. The solid line is the voltage curve after compensating the OV problem, and the dashed line is the voltage curve after

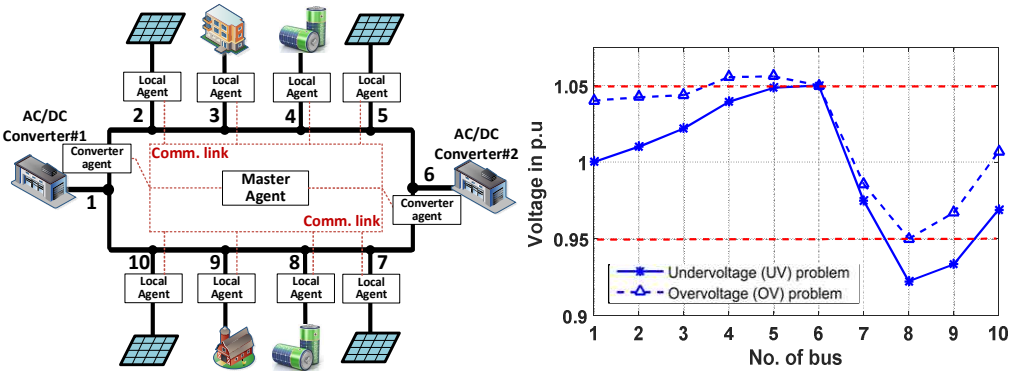

(a) Configuration of control system of multi-terminal LVDC distribution system

(b) Example of voltage profile when overvoltage and undervoltage occur at the same time

Fig. 2. Typical loop-type multi-terminal LVDC distribution system and its voltage profile: (a) configuration of voltage control system using multi-agent system and (b) example of voltage profile when UV and OV problems occur in different feeders

UV problem compensation. It can be seen that both voltage curves exceed the normal range. This indicates that the coordination of multiple AC/DC converters and multiple DERs should be applied to secure voltage control.

3. Proposed Voltage Control Scheme for Multi-terminal LVDC Distribution System

3.1 Objective of proposed voltage control method

This subsection describes the objective and basic principles of the voltage control method proposed in this paper. Based on a power flow analysis, the proposed algorithm adopts a method to cooperatively control multiple AC/DC converters, PV, and BESSs. The goal of voltage control is to keep the distribution voltage stable within 5% of the nominal voltage according to the American National Standards Institute (ANSI) for distribution systems [15].

In AC power distribution systems, the voltage magnitude can be controlled through auxiliary reactive power control but in DC power distribution systems, the voltage must be controlled through active power control. Therefore, voltage control in LVDC distribution system is directly related to electricity price and/or electric power market.

The proposed voltage control method aims to meet the following fundamental objectives:

- To increase the deliverable power ratings and reduce energy losses of the LVDC distribution lines.
- To improve the hosting capacity of DERs in the LVDC distribution system by compensating OV problems caused by additional DERs.
- To consider the generation of renewable energy resources such as PVs as the first priority so that renewable energy sources can produce more power to the system.
- To minimize the discharge energy from BESSs for voltage control. With this concept, we can efficiently use BESS and reduce its rated size.

Based on the above objectives, we develop the coordinated control method for LVDC distribution systems.

3.2 Overview of proposed voltage control method

Fig. 3 shows the flowchart of the overall voltage control method for multi-terminal LVDC distribution systems. After obtaining the initial data about the power system network topology, the control system normally operates in monitoring mode measuring the power system parameters, such as bus voltage, line current, load demand, power injection from DERs, stage-of-charge (SOC) of BESS, and so on. Voltage problem can be detected by calculating the largest voltage violation from the normal range (0.95~1.05 p.u) using (3.1) and (3.2)

$$\Delta V_{UV} = \left|0.95 - V_{\min}\right| \cdot u\left(0.95 - V_{\min}\right) \tag{3.1}$$

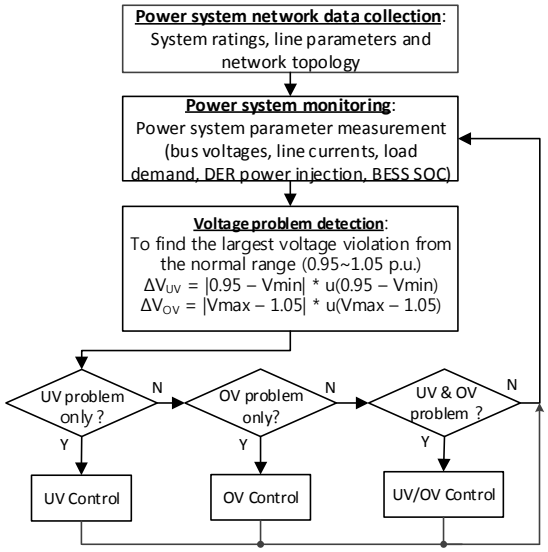

Fig. 3. Flowchart of voltage control scheme in multi-terminal LVDC distribution system

$$\Delta V_{OV} = \left|1.05 - V_{\max}\right| \cdot u\left(V_{\max} - 1.05\right) \tag{3.2}$$

where ΔV_{UV} and ΔV_{OV} are the maximum voltage violations due to UV and OV, respectively; $V_{\min}$ and $V_{\max}$ are the minimum and maximum voltages (in per unit) on the multi-terminal LVDC distribution system, respectively; and the unit-step function, $u(x)$, returns 1 when $x \geq 0$ and 0 when $x < 0$.

The proposed voltage control method can be classified into three categories: i) UV control; ii) OV control and iii) simultaneous UV and OV (UV/OV) control in the different feeders. For each category, we define the detailed control algorithms elaborated on in the following subsections.

3.3 Control algorithm for UV problem

Fig 4 shows the flowchart of the voltage control algorithm for the UV problem, which is a portion of the overall flowchart shown in Fig. 3. To solve the UV problem, it is necessary to increase the power injection from DERs such as PVs and ESSs, and/or increase the output terminal voltage of the AC/DC converters.

The proposed UV control method consists of three major steps to effectively coordinate the AC/DC converters, PVs and BESS. As shown in Fig. 4, the method proposed in this paper selects the PV output increase as a top priority. In general, PVs aim to produce maximum power through MPPT control, but they may produce below the maximum value under certain conditions. In this case, we can increase the PV output to improve the voltage profile. The effect of a generation power increase (ΔP_j) of the PV on the j-th bus in the LVDC distribution system on the voltage of the i-th bus (ΔV_i) can be calculated via the VSF (VSF_{ij}) as

$$\Delta V_i = VSF_{ij} \cdot \Delta P_j \tag{3.3}$$

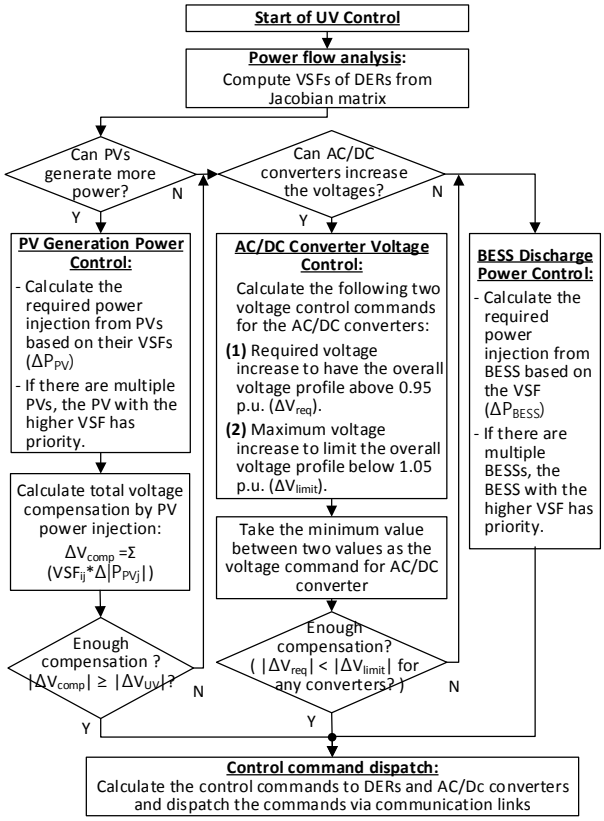

Fig. 4. Voltage control scheme for UV Problem

The method used to obtain accurate VSFs is explained in detail in the next section. If there are multiple PVs in the LVDC distribution system, the voltage compensation (ΔV_{comp}) of the i-th bus through the control of multiple PVs can be obtained by adding each compensated voltage as

$$\Delta V_{comp} = \sum_{j=1}^{N} \left(VSF_{ij} \cdot \Delta P_j \right) \tag{3.4}$$

If voltage compensation using PV is not enough ($\Delta V_{comp} < \Delta V_{UV}$), the voltage profile will still be under the normal range. Then, we should move on to the next step for AC/DC converter control.

The output voltage control of the AC/DC converter is a powerful means of controlling the voltage profile across the whole LVDC distribution system. In general, while the DER power control can shape the local voltage profile curves, the voltage control of the AC/DC converter can affect the voltage profile of the whole LVDC distribution system. This control is similar to the control of the on-line-tap-changer (OLTC) in the AC distribution system but the control accuracy and speed of the AC/DC converter are much higher than those of the OLTC.

When we apply the AC/DC converter control, we need to check if the voltage increase for the UV control of the AC/DC converter may cause OV problems on the other buses in the distribution system. As shown in Fig. 4, we should calculate the following two voltage control commands: i) the required voltage increase of the AC/DC converter (ΔV_{req}) to keep the overall voltage profile above 0.95 p.u. and ii) the maximum voltage increase ($\Delta V_{\lim it}$) to limit the overall voltage profile below 1.05 p.u. The detailed procedure used to calculate the exact voltage control commands for AC/DC converters is described in the next section. If the first value (ΔV_{req}) is smaller than the second (ΔV_{limit}), the AC/DC converter control can fully compensate UV problem of the whole system without causing OV problems in the other buses. If not, the AC/DC converters will not allow enough compensation for the UV problem. Then, we should try the last control action using BESSs.

BESSs can be installed for multiple purposes such as peak shaving, arbitrage transaction, renewable energy integration and voltage control. Since the storage capacity of the BESS has a large effect on the installation cost, we need to save the stored energy in the BESS for voltage control in the last stage.

The principle of voltage control using BESS is similar to that of PV because both PV and BESS can compensate the voltage by controlling the injection power. It is effective to preferentially control the BESS installed at a position where the VSF is large. The difference with PV is that PVs usually operate in the MPPT mode so that the margin of power available for UV control may be insufficient, while BESSs have a relatively large amount of energy available for voltage control.

3.4 Control algorithm for OV problem

Fig. 5 shows the flowchart of the control algorithm for the OV problem. As with UV control, we coordinate the AC/DC converters, BESSs and PVs in sequence, but the control priority for the proposed OV control differs from that for the UV control method. Normally, OV can occur when DERs, such as PVs, inject excessive power to the distribution system, especially under light loading conditions. As shown in Fig. 5, the proposed coordinate control sequence is as follows: i) reduce BESS discharge, ii) charge electric power to BESSs if PVs generate excessive power to the line, iii) reduce the voltage of the AC/DC converter, and iv) finally, reduce the power generation of PVs.

If there are discharging BESSs in the distribution system, the first control action is to reduce BESS discharging. Then, we can calculate how much voltage can be reduced by this first control action using (3.3).

If there is PV generation power to the LVDC distribution line, it can cause OV problem in the line. Therefore, in the second step, we charge the BESSs with the PV generation power. Then, we can maximally use the PV generation even during OV problems. To this end, calculate the amount of power to charge in the BESS for the required voltage reduction. If there are multiple BESSs in the LVDC system, the BESS with the higher VSF has the priority to charge the power first. By considering the VSFs and SOCs

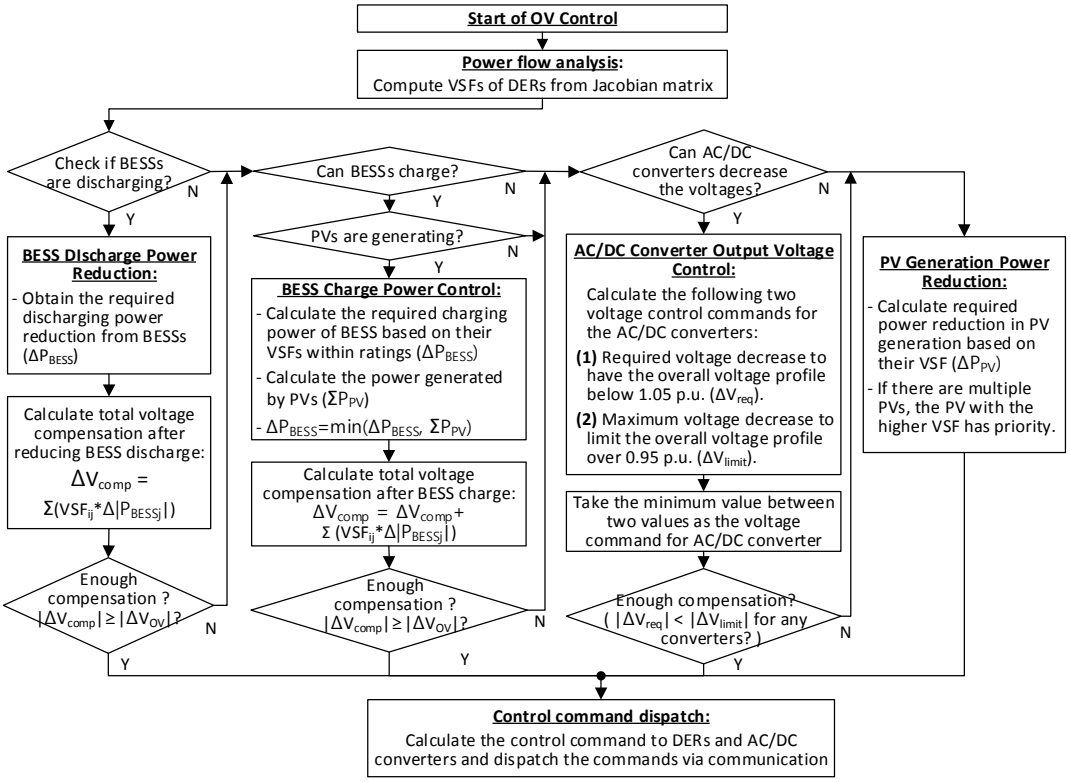

Fig 5. Voltage control scheme for OV problem

of BESSs, we can calculate the exact amount of charging power of BESSs.

AC/DC converter control is considered when the first two actions cannot maintain the voltage profiles within the normal range. In this control action, we need to ensure that the voltage decrease of AC/DC converters control does not cause UV problems in other feeders. To this end, we compute the two voltage commands: i) the required voltage decrease to limit the overall voltage profile below 1.05 p.u. (ΔV_{req}), and ii) the maximum voltage decrease to have the overall voltage profile over 0.95 p.u. (ΔV_{limit}). If the second voltage command is higher than the first voltage command, the AC/DC converters have enough capacity to reduce the maximum voltage without causing UV problems in any feeders. If not, we need to reduce the PV power generation at the final step.

One of the major reasons for OV problems is excessive power injection from DERs. Therefore, if we can reduce the power injection from PVs, OV problems can be solved in most cases. The control procedure for PV power control is similar to that for UV control. The PV with the higher VSF value is applied first until the required voltage compensation can be achieved.

3.5 Control algorithm for simultaneous occurrence of UV and OV problems

Fig. 6 shows the voltage control scheme when the UV and OV problems occur in different feeders at the same

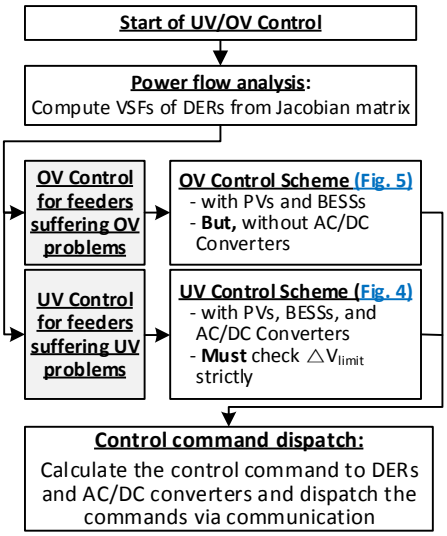

Fig. 6. Voltage control scheme if OV and UV occur at same time

time. For the feeders suffering from the OV problem, the control procedure is similar to the OV control in Fig. 5, but the AC/DC converters are not considered because they cause the additional voltage drop in UV-feeders. In the feeders suffering from the UV problem, the control procedure is almost the same as the UV control in Fig. 4. In the UV control, it must be checked if the maximum voltage is lower than 1.05 p.u. after the voltage increase in the UV feeder.

4. Calculation of Control Commands for AC/DC Converters and DERs

Section 3 discussed the voltage control principle through the cooperation of AC/DC converters, PVs, and BESSs. This section describes how to calculate the control commands for DERs and AC/DC converters in detail.

4.1 VSFs for DERs

The VSF is defined as the effect of the power variation control of the DERs on the voltage compensation of a specific bus. Therefore, we can determine the control priority based on the VSF values of DERs.

[18] proposed that VSF can be obtained from the Jacobian matrix of the LVDC distribution system. We can define the VSF between the voltage at the *i*-th bus and the power injection at the *j*-th bus as

$$\left[VSF\right]_{ij} = \frac{\Delta V_i}{\Delta P_j} = \left[J\right]_{ij}^{-1} \tag{4.1}$$

where *J* is the Jacobian matrix corresponding to derivations of the active power from the bus voltage magnitude. The full equation of Jacobian matrix is obtained as follows:

Off-diagonal elements:

$$J_{ij} = V_i G_{ij} \tag{4.2}$$

Diagonal elements:

$$J_{ii} = 2V_i G_{ii} + \sum_{j=1, j\neq i}^{N} V_j G_{ij} \tag{4.3}$$

where N is the number of buses, V_i and V_j are the bus voltages at the *i*-th and *j*-th nodes, respectively. The bus conductance matrix G is defined as

$$G = \begin{bmatrix} G_{11} & G_{12} & \cdots & G_{1n} \\ G_{21} & G_{22} & \cdots & G_{2n} \\ \cdots & \cdots & \ddots & \cdots \\ G_{n1} & G_{n2} & \cdots & G_{nn} \end{bmatrix} \tag{4.4}$$

$$G_{ii} = \sum_{j=1}^{n} g_{ij} \quad \text{and} \quad G_{ij}\big|_{i\neq j} = -g_{ij} \tag{4.5}$$

where g_{ij} is the conductance of the line between *i*-th and *j*-th buses. The conductance matrix is similar to the bus admittance matrix for an AC distribution system and the only difference is absence of reactance components.

Then, the equation for determining the DER output power can be derived as

$$\Delta P_j = \frac{\Delta V_k}{VSF_{kj}} \tag{4.6}$$

where, bus *k* is the target bus for voltage control and *j* is the bus index where the selected DER is connected. The variable ΔV_k represents the voltage deviation of the target bus from the normal range and ΔP_j is the required additional power injection from the DER at the *j*-th bus.

To adjust the output of the DERs, the power margin should be considered for voltage compensation using DER control. The power margin of a DER can be obtained by subtracting the output power from the rated power. The control commands for the power output of DERs must be smaller than the power margin.

4.2 Control commands for AC/DC converters

In this section, we propose a method to coordinate multiple AC/DC converters for voltage control for multi-terminal LVDC distribution systems and to calculate the exact voltage control commands for AC/DC converters.

The first step is to determine the order of control priority of the AC/DC converters. The fundamental idea is to give the AC/DC converters with better control performance a higher priority. We can use the electrical distance between the AC/DC converter and the control target bus as the control performance. Here the electrical distance can be represented by the resistance of the line. The process is summarized as follows.

- Obtain the lengths of the distribution lines from the database of the central controller
- Calculate the line resistance between the AC/DC converter and the target bus using the information of the corresponding line.
- Give the AC/DC converters with lower line resistance control priority.

If the first-chosen AC/DC converter cannot fully compensate the target bus voltage, the second converter is activated to restore the voltage within the normal range. This process is repeated until the last AC/DC converter reaches its limited output voltage.

The next step is to determine the control commands for AC/DC converters in multi-terminal LVDC distribution systems. To obtain the output voltages of the AC/DC converters, we propose two methods in this paper. In the first method, the power flow analysis should be performed to analyze the influence of the voltage change at the specific bus on the voltage control in the other bus. In particular, the control commands of the output voltage of the AC/DC converter are calculated through iterative numerical analysis.

If the nonlinear characteristics of the load are neglected, the distribution system can be approximated by linearization circuit model so that the superposition theory can be applied to the system. The second method finds the control commands of AC/DC converters by using linear circuit theory after considering the equivalent resistance model of the loads.

The two methods proposed in this paper are described

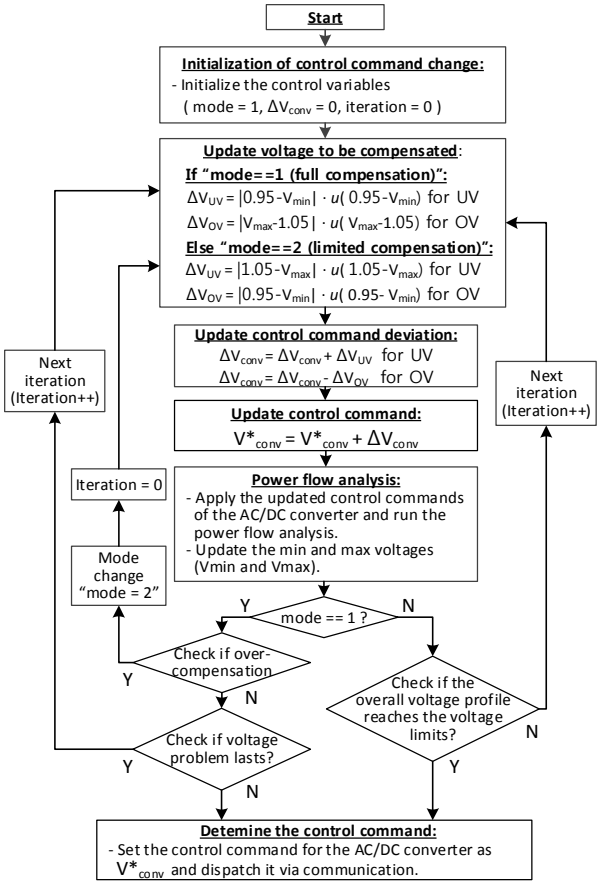

Fig. 7. Procedure of iterative numerical computation method

below. The performance of the two methods is compared and analyzed in Section 5.

4.2.1 Method 1: Iterative numerical computation method

This method calculates the converter control commands using iterative computation based on the concept of the Gauss-Seidel method that can reduce the computation error iteratively. Fig. 7 shows the procedure of this method, and the details of the calculation procedure are as follows:

Step 1: The control system selects the AC/DC converter among multiple AC/DC converters according to the control priority. There are two modes of operation. The full-compensation mode (mode 1) is fully to compensate the OV problem to the normal range. The limited compensation mode (mode 2) restrict the voltage control command to prevent UV problem in other feeder.

Step 2: Update the compensation voltage with Eqs. (3.1) and (3.2) for mode 1 and Eqs. (4.7) and (4.8) for mode 2. Eq. (4.7) represents the maximum voltage increase to limit the overall voltage below 1.05 p.u. for UV control. Similarly, Eq. (4.8) represents the maximum voltage reduction to keep the overall voltage above 0.95 p.u. for the OV problem

$$\Delta V_{UV} = \left|1.05 - V_{\max}\right| \cdot u\left(1.05 - V_{\max}\right) \tag{4.7}$$

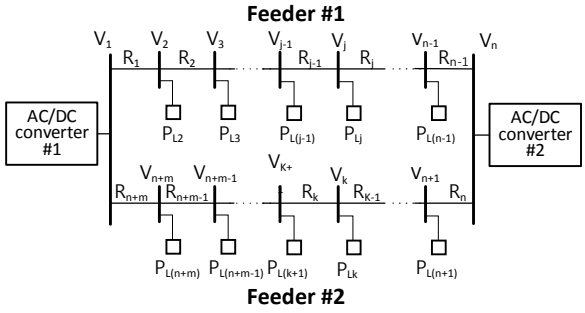

Fig 8. Power system parameters in multi-terminal LVDC distribution system

$$\Delta V_{OV} = \left|0.95 - V_{\min}\right| \cdot u\left(0.95 - V_{\min}\right) \tag{4.8}$$

Step 3: Apply the update control command of the AC/DC converter and run the power flow analysis for the whole LVDC distribution system. Then, update the overall voltage profiles of the system.

Step 4: If the maximum and minimum voltages are within the normal range during mode 1 operation or the maximum/minimum voltage reaches the lower limit of the normal range in during mode 2 operation, the algorithm stops and the output voltage command for the corresponding AC/DC converter is determined. Otherwise, go to step 2 and go through more iterations.

4.2.2 Method 2: Linearly approximated circuit analysis

This method calculates the control commands of AC/DC converters based on the linear circuit analysis. To calculate the control commands, let us define the node voltages at the (j-1)-th and j-th buses as V_{j-1} and V_j, respectively, and the resistance between the (j-1)-th and j-th buses as R_{j-1}, as illustrated in Fig. 8.

The load in Fig. 8 can be rendered as a resistance model as

$$R_{Lj} = \frac{V_{rated}^2}{P_{Lj}} \tag{4.9}$$

where V_{rated} is the rated voltage of the LVDC distribution system and P_{Lj} is the load power consumption at bus j measured from the local agent. For example, when applying Kirchhoff's Current Law (KCL) to the node 2 in Fig. 8, we can obtain the voltage equation as

$$\left(\frac{1}{R_1} + \frac{1}{R_2} + \frac{1}{R_{L2}}\right) \cdot V_2 - \frac{1}{R_2} \cdot V_3 = \frac{1}{R_1} \cdot V_{conv\#1} \tag{4.10}$$

Similarly, applying KCL to the arbitrary j-th node in feeder#1 yields

$$\frac{1}{R_{j-1}} \cdot V_{j-1} - \left(\frac{1}{R_{j-1}} + \frac{1}{R_j} + \frac{1}{R_{Lj}}\right) \cdot V_j + \frac{1}{R_j} \cdot V_{j+1} = 0 \tag{4.11}$$

$$\begin{bmatrix} \left(\frac{1}{R_1}+\frac{1}{R_2}+\frac{1}{R_{L2}}\right) & -\frac{1}{R_2} & 0 & \cdots & 0 \\ \frac{1}{R_2} & -\left(\frac{1}{R_2}+\frac{1}{R_3}+\frac{1}{R_{L3}}\right) & \frac{1}{R_3} & \cdots & 0 \\ \vdots & \vdots & \vdots & \vdots & \vdots \\ 0 & 0 & 0 & -\frac{1}{R_{n-2}} & \left(\frac{1}{R_{n-2}}+\frac{1}{R_{n-1}}+\frac{1}{R_{L(n-1)}}\right) \end{bmatrix} \begin{bmatrix} V_2 \\ V_3 \\ \cdots \\ \cdots \\ V_{n-1} \end{bmatrix} = \begin{bmatrix} \frac{1}{R_1}V_{conv\#1} \\ 0 \\ \cdots \\ 0 \\ \frac{1}{R_{n-1}}V_{conv\#2} \end{bmatrix} \tag{4.12}$$

$$\begin{bmatrix} \left(\frac{1}{R_n}+\frac{1}{R_{n+1}}+\frac{1}{R_{L(n+1)}}\right) & -\frac{1}{R_{n+1}} & 0 & \cdots & 0 \\ \frac{1}{R_{n+1}} & -\left(\frac{1}{R_{n+1}}+\frac{1}{R_{n+2}}+\frac{1}{R_{L(n+2)}}\right) & \frac{1}{R_{n+2}} & \cdots & 0 \\ \vdots & \vdots & \vdots & \vdots & \vdots \\ 0 & 0 & 0 & -\frac{1}{R_{n+m-1}} & \left(\frac{1}{R_{n+m-1}}+\frac{1}{R_{n+m}}+\frac{1}{R_{L(n+m)}}\right) \end{bmatrix} \begin{bmatrix} V_{n+1} \\ V_{n+2} \\ \cdots \\ \cdots \\ V_{n+m} \end{bmatrix} = \begin{bmatrix} \frac{1}{R_n}V_{conv\#2} \\ 0 \\ \cdots \\ 0 \\ \frac{1}{R_{n+m}}V_{conv\#1} \end{bmatrix} \tag{4.13}$$

Then, we can derive the equation that explains the relationship between the bus voltages, line resistances, and bus load resistances as (4.12), which can be calculated from (4.9). Similarly, we can obtain the voltage equation for feeder#2 as (4.13).

If we assume that bus *j*-th is the target bus, we can get the voltage at the target bus following as a function of the voltage at the AC/DC converters from (4.12) as

$$\alpha \cdot V_{conv1} + \beta \cdot V_{conv2} = \gamma \cdot V_j \tag{4.14}$$

where α, β, and γ are the coefficients formed by line and load resistance. The values of the coefficients for the case study in this paper are summarized in Appendix A

In AC/DC converter control, if one converter is chosen for the compensating voltage problem in the feeders, the others will be kept constant. When we control the output voltage of AC/DC converter#1 and maintain the voltage of AC/DC converter#2, we obtain

$$\alpha \cdot \Delta V_{conv1} = \gamma \cdot \Delta V_j \tag{4.15}$$

where $\Delta V_{conv1} = V_{conv1}^{new} - V_{conv2}^{old}$ and $\Delta V_j = V_j^{new} - V_j^{old}$. Finally, we can obtain the control command of the AC/DC converter#1 as

$$\Delta V_{conv1} = \frac{\gamma}{\alpha} \cdot \Delta V_j \tag{4.16}$$

Similarly, we can calculate the voltage control command of AC/DC converter#2 as

$$\Delta V_{conv2} = \frac{\gamma}{\beta} \cdot \Delta V_j \tag{4.17}$$

5. Case studies

5.1 Test system for simulation case studies

To verify the performance of the proposed voltage control scheme, we use a simulation model of a multi-terminal LVDC distribution system using MATLAB as shown in Fig. 9. The simulation model has two AC/DC converters that interconnect the multi-terminal LVDC system to the 22.9-kV medium-voltage AC grids and is configured as a loop system with 10 buses. The distribution line is modeled as overhead line used in South Korea such as OW 60 mm^2, with line resistance of 0.313 Ω/km. The configuration of the multi-terminal LVDC distribution system is a bipolar system whose rated voltage between two poles is DC 1,500V as explained in [4]. The distance and resistance of the distribution line are listed in Table 1.

Then, we assume various loading conditions as listed in Table 2. The loading conditions can be classified into several categories as follows:

- **Normal loading condition (L0)**: In this condition, the overall voltage profile can be maintained within the normal range because loads are moderate.
- **Heavy loading conditions (L1 and L2)**: In these conditions, the UV problem occurs due to load increase in feeder#1 with 40% increase in L1 and 100% in L2 compared to L0
- **Heavier loading conditions (L3 and L4)**: The loads in feeder#1 are increased more than heavy-loading condition L1 and L2. Therefore, the multi-terminal LVDC distribution system suffers severe UV problems.

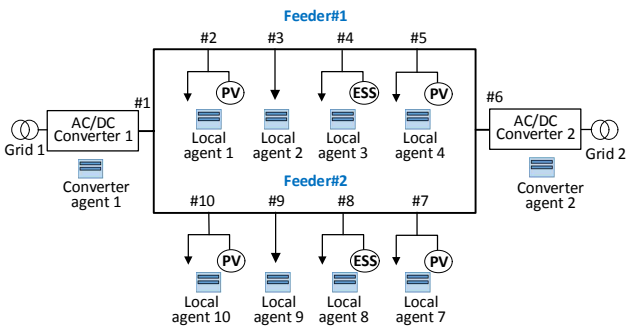

Fig. 9. Configuration of the test system for multi-terminal LVDC distribution system

Table 1. Line parameters of the test multi-terminal LVDC distribution system

From bus	To bus	Line length and resistance		
		Distance	Resistance	
		in km	in Ω	in p.u.[1]
1	1	2.5	1.5650	0.0696
1	10	0.75	0.4695	0.0200
2	3	3.5	2.1910	0.0974
3	4	1.75	1.0955	0.0487
4	5	2.75	1.7125	0.0765
5	6	2.45	1.5337	0.0682
6	7	2.25	1.4085	0.0626
7	8	3.5	2.1910	0.0974
8	9	1.45	0.9077	0.0403
9	10	1.25	0.7825	0.0348

[[1] Base values: V_{base} = 1,500 V, P_{base} = 100 kW]

Table 2. Loading conditions for case studies [Unit: kW]

Load / Bus	Case 1					Case 2		Case 3
	L0	L1	L2	L3	L4	L5	L6	L7
1	-	-	-	-	-	-	-	-
2	9	12.6	18	22.5	27	5.4	2.7	2.7
3	12	16.8	24	24	36	7.2	3.6	3.6
4	27	37.8	54	54	81	16.2	8.1	8.1
5	15	21	30	30	45	9.0	4.5	4.5
6	-	-	-	-	-	-	-	-
7	25	25	25	25	25	25	25	60
8	40	40	40	40	40	40	40	90
9	25	25	25	25	25	25	25	60
10	15	15	15	15	15	15	15	40
Total	168	193.2	231	262.5	294	142.8	123.9	368.9

- **Sudden load decrease during UV control (L5 and L6)**: The loads in feeder#1 decrease suddenly with 80% in L5 and 90% in L6 compared to L4. Then, OV problems occur on feeder#1.
- Heavy **loading and light loading conditions in different feeders (L7)**: The loads in feeder#1 are high, while the loads in feeder#2 are low. Then the LVDC system can simultaneously suffer both the UV and OV problems in different feeders. In this case, coordination controls between DERs and AC/DC converters are significant as described in Fig. 6.

5.2 Comparison of control performance of the AC/DC converter

Here, we evaluate the control performance of the AC/DC converters in terms of their electrical distance and the methods to determine the control command of the converters. The evaluation is based on simulation studies under L2 loading condition of the test system.

First, we evaluate the control performance of the AC/DC converter based on their electrical distance to the target bus. When we have multiple converters in a multi-terminal LVDC distribution system, we can decide the control priority of the converters based on electrical distance between the target bus and the AC/DC converters, as

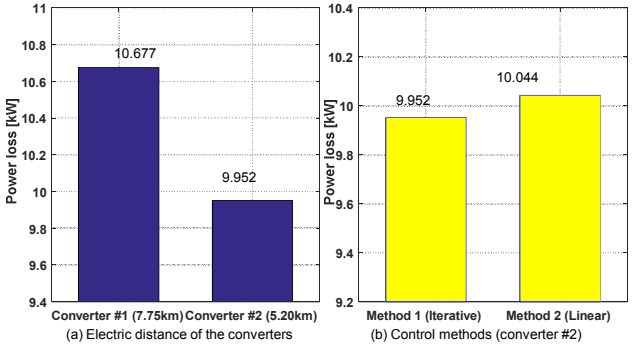

Fig. 10. Power losses comparison: (a) between two converters; and (b) between two control methods

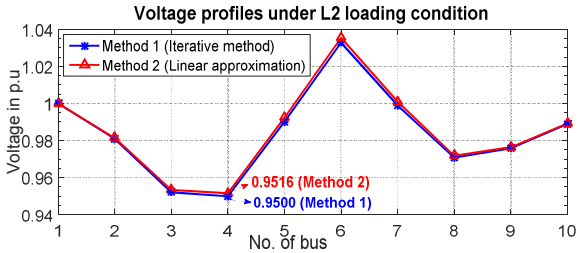

Fig. 11. Voltage profile after UV compensation of the two methods in L2 condition

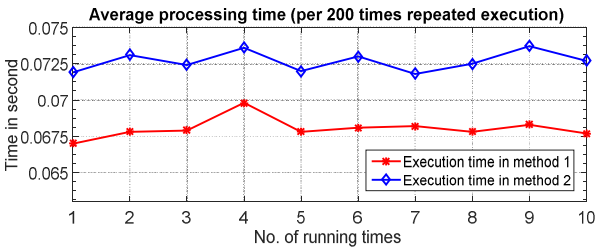

Fig. 12. Comparison processing time between the two methods

explained in Section 4.2. During the L2 loading condition, the LVDC distribution system suffers the UV problem and the minimum voltage occurs at bus 4. As listed in Table 1, the electrical distance to AC/DC converter #2 (5.20km) is shorter than AC/DC converter #1 (7.75km). Therefore, we can give higher control priority to AC/DC converter#2 than to converter #1. Fig. 10(a) shows the power losses in the LVDC distribution line when each AC/DC converter compensates the UV problem at bus 4. It can be seen that the UV compensation using the AC/DC converter #2 is more efficient than using converter #1, which supports our rule of converter selection.

Second, we examine the control performance of the AC/DC converters based on the method to determine the control command of the converters. In Section 4, we presented two methods to determine the voltage control command of AC/DC converter using iterative numerical computation (method 1) and linearly approximated circuit analysis (method 2). Fig. 10(b) compares the power loss

when the two methods are applied to the same UV compensation at L2 loading condition. It can be noted that method 1 is more efficient than method 2. This is because the computation of the voltage control command of method 1 is more accurate than that of method 2.

Fig. 11 compares the voltage profile after UV compensation of the two methods in L2 condition. The minimum voltage is compensated to 0.95 p.u. in method 1 and 0.9561 in method 2. It can be noted that method 1 is more accurate than method 2 because the control objective is to restore the minimum voltage to 0.95 p.u.

Fig. 12 compares the computation time in two methods to calculate the voltage control commands for the AC/DC converters. To obtain the results, we implemented the control algorithms including the two methods and the power system model of the test LVDC distribution system. We tested the processing time by running and compiling the codes 200 times. Normally, iterative computation takes longer than a deterministic equation to get solutions; however, the results in Fig. 12 indicates that the computation times of the two methods are similar to each other, each having average values of about 0.07 seconds. This because the LVDC distribution system is relatively simple for method 1 and the equations in method 2 are complicated. Randomness shown in Fig. 12 is due to other background procedure of operating system in computer.

According to the above comparison results in terms of accuracy, power losses, and processing time, we can conclude that method 1 is more suitable to compute the AC/DC converter command in this simulation studies. Therefore, in the following case studies, we will apply method 1 to obtain the control command of the AC/DC converters.

5.3 Case 1: UV problem in feeder#1

In this case, we assume five different loading conditions (L0 to L4) as described in Table 2. Table 3 lists the voltage profile under each loading condition before any control actions. The second column in Table 3 indicates the voltage profile during normal loading condition L0. In this condition, the minimum voltage is 0.9584 p.u., which is in the normal range. The third to sixth columns show the voltage profiles under L1, L2, L3, and L4 loading conditions, respectively. The voltage at bus 4 is the lowest in all loading conditions; thus, bus 4 will be selected as the target bus for UV control.

Table 3. Voltage profile under each loading condition [Unit: p.u]

Bus	L0	L1	L2	L3	L4
1	1.0000	1.0000	1.0000	1.0000	1.0000
2	0.9803	0.9720	0.9590	**0.9477**	**0.9358**
3	0.9616	**0.9454**	**0.9200**	**0.8976**	**0.8739**
4	0.9584	**0.9408**	**0.9132**	**0.8888**	**0.8631**
5	0.9749	0.9643	**0.9477**	**0.9331**	**0.9178**
6	1.0000	1.0000	1.0000	1.0000	1.0000
7	0.9738	0.9738	0.9738	0.9738	0.9738
8	0.9580	0.9580	0.9580	0.9580	0.9580
9	0.9683	0.9683	0.9683	0.9683	0.9683
10	0.9861	0.9861	0.9861	0.9831	0.9831

Table 4 shows the voltage profile after PV generation power control. Let us focus on the L1 loading condition first. The third column in Table 4 explains the voltage profiles in L1 after using PV control. Table 5 lists the VSFs of the buses in feeder#1 against the target bus 4. There are two PVs installed in feeder #1 at buses 2 and 5. The PV located at bus 5 will be selected first for voltage control action given the higher VSF than bus 2. The required power injection from the PV at bus 5 is computed as 20.4520 kW according to (4.6), but it must be limited to 20kW because of the rated power of the PVs. Therefore, the PV located at bus 2 need to be selected to generate an additional 1.0296 kW according to (4.6) to keep the voltage within the normal range.

The red dashed line in Fig. 13 shows the voltage profiles before control action and the green line is the voltage profile after PV control for L1 loading condition. As shown Table 4, the PV control cannot bring the minimum voltage

Table 4. Voltage profiles after PVs generation power control under each loading condition [Unit: p.u]

Bus	L0	After PV control			
		L1	L2	L3	L4
1	1.0000	1.0000	1.0000	1.0000	1.0000
2	0.9803	0.9755	0.9740	0.9630	0.9516
3	0.9616	0.9528	**0.9355**	**0.9138**	**0.8909**
4	0.9584	0.9500	**0.9288**	**0.9052**	**0.8803**
5	0.9749	0.9761	0.9627	**0.9487**	**0.9339**
6	1.0000	1.0000	1.0000	1.0000	1.0000
7	0.9738	0.9738	0.9738	0.9738	0.9738
8	0.9580	0.9580	0.9580	0.9580	0.9580
9	0.9683	0.9683	0.9683	0.9683	0.9683
10	0.9861	0.9861	0.9861	0.9861	0.9861

Table 5. VSFs of buses in Feeder#1 to bus 4 under L1 loading condition

Bus	VSF Values
2	0.0307
3	0.0754
4	0.0971
5	0.0450

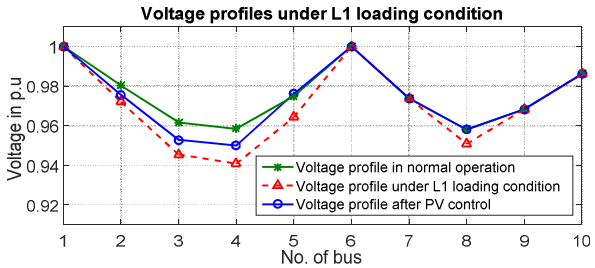

Fig. 13. Voltage profiles under L1 loading condition with and without coordinated voltage control

Table 6. Voltage profiles before and after control actions under loading conditions [Unit: p.u]

Bus	PVs and converter#2 control			PVs and two converters #1 and #2 control		PV and two converters and BESS control
	L2	L3	L4	L3	L4	L4
1	1.0000	1.0000	1.0000	1.0261	1.0500	1.0500
2	0.9809	0.9739	0.9628	0.9954	1.0044	1.0086
3	0.9521	0.9398	0.9179	0.9549	0.9474	0.9573
4	0.9500	0.9383	0.9145	0.9500	0.9374	0.9500
5	0.9901	0.9910	0.9769	0.9965	0.9878	0.9938
6	1.0328	1.0500	1.0500	1.0500	1.0500	1.0500
7	0.9990	1.0122	1.0122	1.0190	1.0251	1.0251
8	0.9708	0.9776	0.9776	0.9946	1.0101	1.0101
9	0.9758	0.9797	0.9797	1.0007	1.0199	1.0199
10	0.9889	0.9904	0.9904	1.0146	1.0368	1.0368

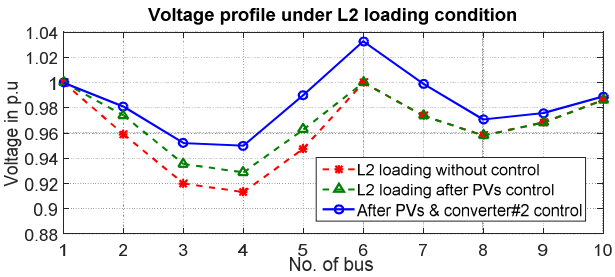

Fig. 14. Voltage profiles under L2 loading condition with and without coordinated voltage control

to the normal range for L2, L3, and L4 loading conditions. According to the algorithm in Fig. 4, the next control step is the AC/DC converter control and BESS control.

Table 6 shows the results for voltage profiles after voltage control actions: 1) PVs and converter #2 control for L2 loading condition, 2) PVs and two converters control under L3 loading condition, and 3) PVs, two converters, and BESS control under L4 loading condition.

Fig. 14 shows the voltage profiles before and after voltage control actions in L2 loading condition. Before any control actions, the minimum voltage is 0.9132 p.u. at bus 4, which violates the normal range. After PV power control, the minimum voltage is restored to 0.9288 p.u. but is still lower than the normal range. Finally, the AC/DC converter #2 boosts its output voltage up to 1.0328 p.u to compensate the bus 4 voltage to 0.9500 p.u.

The voltage profiles before and after control actions in L3 loading condition is given in Fig. 15. Before the control actions, the minimum voltage is as low as 0.8976 p.u. at bus 4. The, this voltage is restored to 0.9052 p.u. after PV control and to 0.9383 p.u. after consecutive AC/DC converter #2 control. Finally, the AC/DC converter #1 increases the bus 1 voltage to 1.0261 p.u. so that the bus 4 voltage becomes 0.9500 p.u. as shown in the blue solid line in Fig. 15.

In L4 loading condition, the voltage at bus 4 dropped to 0.8631 p.u. before control actions. After the PVs and AC/DC converter control, the voltage at bus 4 increase to

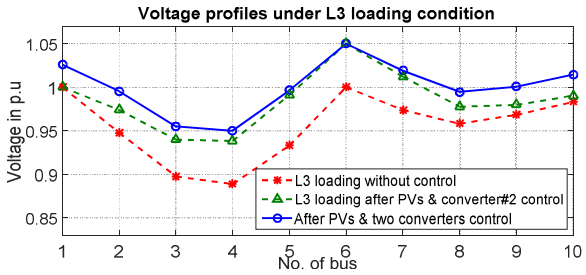

Fig. 15. Voltage profiles under L3 loading condition with and without coordinated voltage control

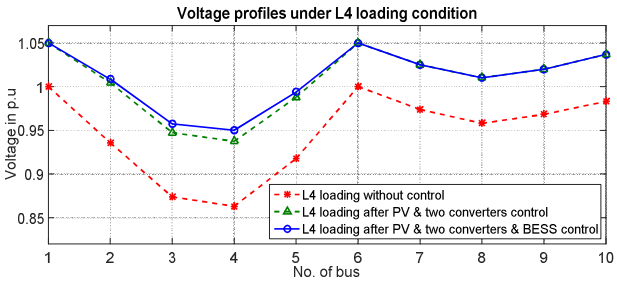

Fig. 16. Voltage profiles under L4 loading condition with and without coordinated voltage control

0.9374 p.u. but it is still lower than the normal voltage range. Therefore, BESSs becomes the last choice for the voltage control algorithm. In this case, BESS located at bus 4 discharge power is as much as 12.322kW according to (4.2). Fig. 16 shows the voltage profiles in L4 loading condition. After the final BESS control, the minimum voltage at bus 4 becomes 0.9500 p.u., as shown in the blue line in Fig. 16.

5.4. Case 2: OV problem in feeder#1

OV problems can occur when DERs inject power to the distribution system during light loading condition. To simulate OV problems, we apply sudden load change from L4 loading condition to L5 or L6 loading condition. In the last simulation in L4 loading condition in case 1, both the AC/DC converters #1 and #2 support the terminal voltage at 1.05 p.u., while the two PVs at buses 2 and 5 generate maximum power up to 20kW and the BESS at bus 4 discharge power to the LVDC distribution system is as much as 12.322kW. At that moment, the load drops 80% (in L5) or 90% (in L6) from L4 loading condition. Then, OV occurs at bus 2 in L5 loading conditions and buses 2, 3, 4, and 5 in L6 loading conditions, as listed in the second and fifth columns in Table 7.

According to the OV control scheme illustrated in Fig. 5, the control priority is the BESS, the AC/DC converter, and the PV in order. Because the BESS discharges 12.322kW when the OV problem occurs, the first control action is to cut off the BESS injection power. If the OV problem persists after the BESS charging is stopped, BESS charging

control should be performed. The amount of charging power can be calculated according to VSFs by (4.6). Table 7 lists the voltage profiles after these BESS control actions. As a result, the OV problem disappears in L5 loading condition but not in L6 condition.

In L5 condition, the required charging power of the BESS at bus 4 is obtained as 8.2564 kW according to the corresponding VSF. Then, as shown in the third column in Table 7, the voltage profile can be maintained in the normal range. If the BESS charges power up to its capacity, which means the SOC of the BESS reaches 100%, then the AC/DC converter needs to control the terminal voltage to solve the OV problem as explained in Fig. 5. The fourth column in Table 7 shows the voltage profile when the AC/DC converter control is activated after the BESS completes charging. Fig. 17 shows the voltage compensation results in L5 loading condition.

Table 7. Voltage profiles under L5 and L6 loading conditions [Unit: p.u]

Bus	L5 Loading Condition			L6 Loading Condition		
	No Control	BESS Control	BESS & Conv Control	No Control	BESS Control	BESS & Conv Control
1	1.0500	1.0500	1.0472	1.0500	1.0500	1.0472
2	1.0588	1.0500	1.0500	1.0609	1.0523	1.0500
3	1.0498	1.0364	1.0402	1.0603	1.0395	1.0380
4	1.0503	1.0330	1.0389	1.0617	1.0348	1.0337
5	1.0541	1.0450	1.0486	1.0608	1.0482	1.0476
6	1.0500	1.0500	1.0500	1.0500	1.0500	1.0500
7	1.0421	1.0251	1.0244	1.0251	1.0251	1.0244
8	1.0085	1.0101	1.0083	1.0101	1.0101	1.0083
9	1.0187	1.0199	1.0176	1.0199	1.0199	1.0176
10	1.0363	1.0368	1.0342	1.0368	1.0368	1.0342

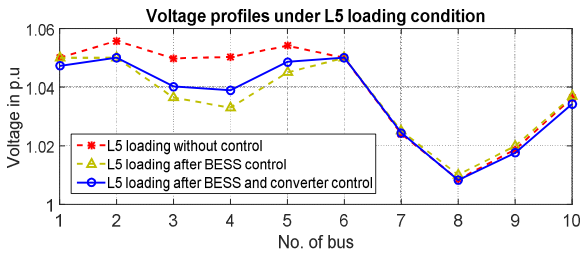

Fig. 17. Voltage profiles under L5 loading condition with and without coordinated voltage control

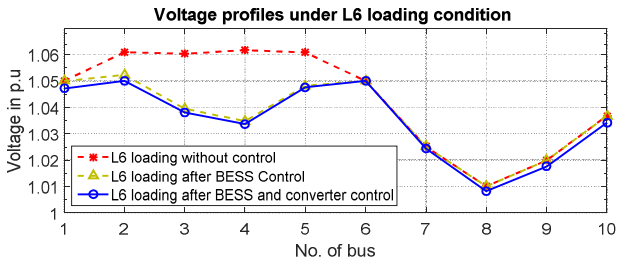

Fig. 18. Voltage profiles under L6 loading condition with and without coordinated voltage control

In L6 loading condition, the sixth column in Table 7 indicates that the BESS control is not enough to compensate for the OV problem. The seventh column in Table 7 shows the voltage profile after the cooperation control of the BESS and the AC/DC converter control. It can be seen that the voltage profile maintains in the normal range. Fig. 18 shows the voltage profiles in L6 loading condition before and after control actions.

5.5. Case 3: Simultaneous OV and UV problem in two different feeders

In this case, we test the voltage control scheme when OV and UV problems occur simultaneously in the different points in the LVDC distribution system. To simulate the case, we assume the following conditions. The outputs of AC/DC converter#1 and converter#2 are operating at 1.03 p.u. and 1.05 p.u. respectively. The two PVs located at buses 2 and 5 generate the maximum power of 20 kW, and the BESS located at bus 4 has discharge power of 12.3223 kW. Then, we apply the L7 loading condition to the LVDC distribution system. On these assumptions, OV problem occurs at buses 4 and 5 in feeder #1 and UV problem occurs at bus 8 in feeder #2 as listed in the second column in Table 8.

To solve these problems, the voltage control follows the control priority in the control procedure shown in Figure 6. First, we stop discharging the BESS on the OV feeder and use PV control on the UV feeder. The third column in Table 8 shows the result of voltage profile when we stop discharging the BESS on bus 4 and PVs located at buses 7 and 10 generate power injection at the maximum value as 20 kW. Because these control actions cannot fully solve the voltage problems, we need to apply BESS charging for the OV feeder to solve the OV problem. The fourth column in Table 8 indicates the voltage profile when the BESS located at bus 4 charges 5.8422 kW, which can reduce the voltage at bus 5 from 1.0523 to 1.0500 p.u.

In feeder #2, there is still UV problem at bus 8 entailing a need to increase the output voltage of the AC/DC

Table 8. Voltage profiles under L7 loading condition [Unit: p.u]

Bus	L7 Loading Condition			
	No Control	BESS cut-off (OV) and PV control (UV)	BESS charging (OV) and PV control (UV)	BESS charging (OV), PV and AC/DC converter control (UV)
1	1.0300	1.0300	1.0300	1.0346
2	1.0449	1.0417	1.0401	1.0432
3	1.0497	1.0418	1.0380	1.0391
4	1.0537	1.0436	1.0387	1.0387
5	1.0571	1.0523	1.0500	1.0500
6	1.0500	1.0500	1.0500	1.0500
7	0.9832	0.9943	0.9943	0.9956
8	0.9387	0.9468	0.9468	0.9500
9	0.9589	0.9655	0.9655	0.9693
10	0.9981	1.0032	1.0032	1.0075

converter to compensate the UV problem. Because the output voltage of AC/DC converter #2 is the maximum voltage 1.05 p.u., AC/DC converter #1 needs to control the output voltage. According to the iterative computation method proposed in Section 4.2.1, we can obtain the voltage increase of AC/DC converter #1 of 0.0046 p.u. This control action brings the voltage at bus 8 from 0.9468 to 0.9500 p.u., which is in the normal range. The last column in Table 8 shows the final voltage profiles after the overall coordinated control.

6. Conclusion and Discussion

This paper presented a voltage control scheme for a multi-terminal LVDC distribution system using the coordination control between multiple AC/DC converters and multiple DERs such as PVs and BESSs. The paper also proposed a method to determine the exact control commands for the AC/DC converters and DERs. The control performance of the proposed voltage control scheme is evaluated via several case studies and analysis of the numerical results.

VSF can be obtained from power flow analysis that requires significant computational resources in the overall control system. Basically, the computation burden for VSF calculation in DC distribution system is less than that of conventional AC distribution system. This is because the size of the Jacobian matrix of DC system is a quarter of AC system (because there is no concept of phase angle and reactive power in DC distribution system). Therefore, the proposed control algorithms for the test cases can be perfectly implemented in 32-bit microcontrollers, which is an affordable solution. However, if we extend the system size to larger complicated LVDC grids, the computation burden and communication delay should be significantly considered. This will be our future research topic in our KEPCO project.

In addition, the accuracy of the proposed algorithm depends on the information on system configuration and real-time measurement data. Therefore, the system information and data must be provided accurately to the control system. The development of autonomous detection procedure of the system configuration and reliable data communication for power system parameter measurement will be significant topic for future study.

Appendix A

The coefficients α, β, and γ of (4.16) ·for buses from 2 to 5 in the simulation cases are listed in Table A.1. The coefficients for buses from 7 to 10 can be obtained similarly.

Table A.1. The coefficients of (4.14) for buses from 2 to 5 in the test simulation cases

Target bus	Coefficients
2	$E = C - \frac{1}{D \cdot R_4^2}$; $F = B - \frac{1}{D \cdot R_3^2}$; $\alpha = \frac{1}{R_1}$; $\beta = \frac{1}{D \cdot E \cdot F \cdot R_2 \cdot R_3 \cdot R_4 \cdot R_5}$; $\gamma = A + \frac{1}{F \cdot R_2^2}$
3	$E = C - \frac{1}{D \cdot R_4^2}$; $\alpha = \frac{1}{A \cdot R_1 \cdot R_2}$; $\beta = \frac{1}{D \cdot E \cdot R_3 \cdot R_4 \cdot R_5}$; $\gamma = B - \frac{1}{A \cdot R_2^2} - \frac{1}{E \cdot R_3^2}$
4	$E = B - \frac{1}{A \cdot R_2^2}$; $\alpha = \frac{1}{A \cdot E \cdot R_1 \cdot R_2 \cdot R_3}$; $\beta = \frac{1}{D \cdot R_4 \cdot R_5}$; $\gamma = C - \frac{1}{E \cdot R_3^2} - \frac{1}{D \cdot R_4^2}$
5	$E = B - \frac{1}{A \cdot R_2^2}$; $F = C - \frac{1}{E \cdot R_3^2}$; $\beta = \frac{1}{R_5}$; $\alpha = \frac{1}{A \cdot E \cdot F \cdot R_1 \cdot R_2 \cdot R_3 \cdot R_4}$; $\gamma = D - \frac{1}{F \cdot R_4^2}$
where $A = \frac{1}{R_1} + \frac{1}{R_2} + \frac{1}{R_{L2}}$; $B = \frac{1}{R_2} + \frac{1}{R_3} + \frac{1}{R_{L3}}$; $C = \frac{1}{R_3} + \frac{1}{R_4} + \frac{1}{R_{L4}}$; $D = \frac{1}{R_4} + \frac{1}{R_5} + \frac{1}{R_{L5}}$;	

Acknowledgements

This research was supported by the KEPCO under the project entitled by "Demonstration Study for Low Voltage Direct Current Distribution Network in an Island," the Global Scholarship Program for Foreign Graduate Students at Kookmin University; and the National Research Foundation of Korea grant funded by the Korea government (NRF-2015R1C1A1A01054635).

References

[1] Starke, M., Tolbert, L.M., Ozpineci, B., "AC vs DC distribution: A loss comparison," *Transmission and Distribution Conference and Exposition, IEEE/PES*, 2008, Chicago, IL, USA, April 22-24.

[2] Whaite, S., Grainger, B., Kwasinski, A., "Power quality in DC distribution systems and microgrid," *Energies*, vol. 8, no. 5, pp. 4378-4399, May, 2015.

[3] Nuutinen, P., Kaipia, T., Peltoniemi, P., Lana, A., Pinomaa, A., Mattsson, A., Silventoinen, P., Partanen, J., Lohjala, J., Matikainen, M., "Research Site for Low-Voltage Direct Current Distribution in a Utility Network - Structure, Functions, and Operation," *IEEE Transactions on Smart Grid*, vol. 5, no. 5, pp. 2574-2582, 2014.

[4] Kim, J., Kim, J., Cho, J., Song, I., Kweon, B., Chung, I., Choi, J., "Comparison between Underground Cable and Overhead Line for a Low-Voltage Direct

Current Distribution Network Serving Communication Repeater," *Energies*, vol. 7, no. 3, pp. 1656-1672, 2014.
[5] Chung, I., Trinh, P.H., Cho, H., Kim, J., Cho, J., Kim, T. "Design and Evaluation of Voltage Control Techniques by Hierarchical Coordination of Multiple Power Converters in Low-Voltage DC Distribution Systems," 2016 CIRED Workshop, Helsinki 14-15 June 2016.
[6] Zhong, Q., Nguyen, P., Ma, Z., Sheng, W. "Self-Synchronized Synchronverters: Inverters without a delicated synchronization unit," *IEEE transactions on power electronics*, vol. 29, no. 2, 2014.
[7] Cairoli, P., Dougal, R.A., Lentijo, K., "Coordination between supply power converters and contactors for fault protection in multi-terminal MVDC distribution systems," *IEEE Electric Ship Technologies Symposium* (*ESTS*), 2013, Arlington, VA, USA.
[8] Chen, D., Xu, L., Zhang, W., "Active distribution system with multi-terminal MVDC links," IEEE Renewable Power Generation (RPG 2015), 2015, Beijing, China.
[9] Monadi, M., Koch-Ciobotaru, C., Luna, A., Candela, J.I., Rodriguez, P., "A protection strategy for fault detection and location for multi-terminal MVDC distribution system with renewable energy systems," IEEE Renewable Research and Application (ICRERA), Milwaukee, Wl, USA, 2014.
[10] Majumder, R., "Aggregation of microgrids with DC system," *Electric Power Systems Research*, vol. 108, pp. 134-143, 2014.
[11] Yang, J., Fletcher, J.E., O'Reilly, J., "Short-circuit and ground fault analyses and location in VSC-based DC networks cable," *IEEE Transactions on Industrial Electronics*, vol. 59, issue 10, pp. 3827-3837, Oct. 2012.
[12] Larruskain, D.M., Zamora, I., Abarrategui, O., Aginako, Z., "Conversion of AC distribution system lines into DC lines to upgrades transmission capacity," *Electric Power Systems Research*, vol. 81, pp. 1341-1348, 2011.
[13] Kweon, B., Chung, I., Kim, J., Cho, J., "Design and operation schemes for battery energy storage systems in low-voltage DC distribution systems considering voltage control and economic feasibility," CRIED, 2015, Lyon, France.
[14] Kang, H., Chung, I., Moon, S., "Voltage Control Method Using Distributed Generators based on a Multi-Agent System," *Energies*, vol. 8, pp. 14009-14025, 2015.
[15] Std, ANSI C84. 1-2011, "American National Standard for Electric Power Systems and Equipment-Voltage Ratings (60 Hertz)," 2011.
[16] Jeong, H., Choi, J., Won, D., Ahn, S., Moon, S., "Formulation and Analysis of an Approximate Expression for Voltage Sensitivity in Radial DC Distribution Systems," *Energies*, vol. 8, no. 9, pp. 9296-9319, 2015.
[17] Hamad, A., Farag, H., El-Saadany, E. A., "Novel Multi-agent Control Scheme for Voltage Regulation in DC Distribution Systems," *IEEE Trans. On Sustainable Energy*, vol. 6, no. 5, pp. 534-545, 2015.
[18] Hai, T.P., Cho, H., Chung, I., Kang, H., Cho, J., Kim, J., "A novel voltage control scheme for low-voltage DC distribution systems using multi-agent systems," *Energies*, vol. 10, doi: 10.3390/en10010041.

Trinh Phi Hai He received his B.E degree in electrical and electronics Engineering from Ho Chi Minh City (HCMC) University of Technology, Ho Chi Minh City, Vietnam in 2012. He is currently working towards his Ph.D degree at Smartgrid Laboratory, Kookmin University, Seoul, Korea. His research interests include multi-agent system application to distribution system, intelligent voltage control schemes for distribution systems and smart grid.

Il-Yop Chung He received B.S., M.S., and Ph.D degrees in electrical engineering from Seoul National University, Seoul, Korea, in 1999, 2001, and 2005, respectively. Currently, he is an Associate Professor at Kookmin University, Seoul, Korea. His research interests are control and operation of power transmission and distribution system, microgrid, and renewable energy resources.

Taehoon Kim He received the B.S. and M.S. degrees in electrical engineering from Kyungpook National University in 2005 and 2007, respectively. Currently, he is working toward Ph.D degree at Hanyang University, Seoul, Korea. He is currently a senior researcher at Basic Research Center for Electric Power of KEPRI (Korea Electric Power Corp. Research Institute), Seoul, Korea. His research interests include DC Microgrid and control algorithm.

Juyong Kim He received the M.S. and Ph.D. degree from Kyungpook National University in 1994 and in 2007, respectively. He joined the KEPRI (Korea Electric Power Corp. Research Institute) as a researcher in 1994. His main research interests are DC distribution system and DC microgrid. He is currently a principal researcher at Smart Power Distribution Lab of KEPRI.